

Impact phenomena of drops of aqueous polymer solution on hot solid

Hitoshi Fujimoto^{1,*}, Kentaro Hamano¹, Takayuki Hama¹, Hirohiko Takuda¹

¹Graduate School of Energy Science, Kyoto University, Kyoto, Japan

*corresponding author: h-fujimoto@energy.kyoto-u.ac.jp

Abstract Quench hardening is extensively utilized to strengthen carbon steel in the metal-forming industries. In this heat treating, submergence methods or spray cooling methods are used to rapidly cool hot materials. Water is commonly employed as the quenchant. Aqueous solutions of water-soluble polymers are also used as typical quenchants. In spray cooling, the impact behavior of the droplets has a great influence on the heat transfer between the hot metal surface and the quenchant. Although there have been numerous experimental studies concerning water droplets, the hydrodynamics of drops of aqueous polymer solutions have been rarely studied. In the present study, the collision of drops of an aqueous polymer solution with a hot sapphire, transparent quartz glass, or metal solid surface, was investigated by means of flash photography. A solution of 10 wt% polyoxyethylene polyoxypropylene glycol, with an average molecular weight of approximately 20,000 was used as the test polymer quenchant. Normal and oblique collisions of drops with a solid were investigated. It was found that the polymer that was in direct contact with the solid spatiotemporally, even when the temperature of the solid was significantly higher than the boiling temperature of water. Additionally, in the case of oblique collisions, the direct contact of the liquid/solid gave rise to an asymmetric motion of drops. The observation techniques and the results will be discussed in detail from an experimental perspective.

Keywords: flash photography, drop of aqueous polymer solutions, boiling

1 Introduction

Quench hardening is extensively utilized to strengthen carbon steels in metal manufacturing industries [1, 2]. During the heat treating, hot carbon steels are rapidly cooled by quenching the medium by means of submergence or through the use of the spray cooling method. Water or oil is commonly used as the quenchant. Water can achieve large heat removal rates from hot materials, giving rise to a large local temperature variation in the hot material. The resultant local thermal stress sometimes leads to unwanted crack initiations or distortion of products. In the case of oil, the heat removal rate is small compared to water. The utilization of oil reduces the possibility of crack initiation of the product. However, its use is associated with a fire hazard, and it leads to bad/worsened/undesirable working conditions in a factory.

As an alternative quenchant type, an aqueous solution of a water soluble polymer is often adopted. The heat transfer rate from hot materials to the polymer solution is smaller than that of water but larger than oil. It can be controlled by both the hydro-dynamical conditions of the quenchant, the chemical components of the polymer, and the concentration of the polymer in the aqueous solution. Although there have been numerous prior experimental studies concerning water droplets [3–5], the hydrodynamics of drops of aqueous polymer solutions have been rarely studied.

In our previous work [6], the collision of drops of an aqueous solution of polymer with a hot sapphire solid surface was investigated as fundamental research of spray cooling in quench hardening. A polymer solution was used as the test quenchant. The incident angle of drops to the solid surface was 90°. We found that the collision behavior of drops of aqueous solutions of water-soluble polymers on hot solid showed similar trends to the behavior of water drops in the film-boiling regime. However, the physics of the phenomena remains unclear.

The objectives of the present study are to experimentally understand the collision behavior of aqueous solution drops of water-soluble polymer with a hot solid. Poxoxyethylene polyoxypropylene glycol with average molecular weight of approximately 20,000 was used as the test polymer. The test solution was made by diluting the test polymer with water into a 10 weight percent mixture. Drops with diameters of approximately 2.3 mm hit a horizontal or a tilted test plate that was heated at 200–500 °C. Sapphire, Inconel alloy 625, or transparent quartz glass (optical prism), were used as the test plate materials. Normal and oblique drop collisions were investigated. For normal drop collisions, the Inconel alloy 625 was adopted.

The results were compared to those in our previous work [6] that used a sapphire plate. For oblique collisions, the sapphire plate was employed to study the effect of the impact angle of the drops to the solid. In addition, the optical quartz prism was applied to observe the liquid/solid contact area during the collision. The observation techniques and the results will be discussed in detail from experimental viewpoints.

2 Test polymer and solution

Polyoxyethylene-polyoxypropylene glycol, with the chemical formula of $\text{HO}-(\text{C}_2\text{H}_4\text{O})_a-(\text{C}_3\text{H}_6\text{O})_b-(\text{C}_2\text{H}_4\text{O})_c-\text{H}$, was adopted as the test polymer. The exact composition was determined by the ratio of $a+c$ to b , which was ranged from 75 to 25. The average molecular weight was approximately 20,000. Figure 1 shows the thermo-gravimetric curve of the test polymer. The figure represents the time variation of the weight of the test polymer when it was heated at the heating rate of 5 °C/min from room temperature to approximately 700 °C. The weight of the test polymer was slightly decreased with increases in the temperature, when the temperature was lower than 300 °C. Sharp decreases of the weight occurred in the temperature range between 300 and 400 °C because the test polymer was decomposed into small molecular weight gases like aldehyde, ketone, or carbon dioxide. Thermal decomposition of the test polymer arose at much higher temperatures than the boiling temperature of water. At temperatures higher than 500 °C, no test polymer remained.

The test solution was made by diluting the polymer with distilled water to 10 wt%. The test solution was transparent and colorless at room temperature. When the test solution was heated above 75 °C (cloud point) [7], the test solution became clouded owing to the difference in the refractive indices of each liquid.

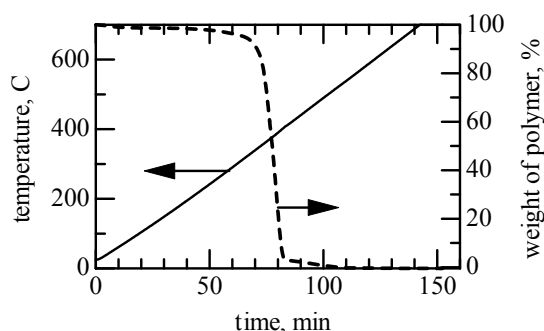


Fig. 1 Thermo-gravimetric curve of test polymer

3 Experiments

In the present study, two types of experiments were conducted. One experiment was conducted to observe the time evolution of the shape of drops on a hot solid. The other experiment was conducted to observe the time evolution of the solid/liquid contact area during the drop collision. These experimental setups are shown in Figures 2 and 3. In both experiments, the flow visualization was realized by means of strobe photography.

3.1 Experimental apparatus for observing the deformation behavior of drops

Figure 2 shows a schematic diagram of the experimental apparatus used to observe the impact phenomena of drops on the heated surface. Since the setup and the measurement procedure were similar to those used in our previous work [6], they are explained briefly. Drops with diameters of approximately 2.3 mm were formed at the nozzle. The drops at room temperature fell and hit a horizontal or a tilted test piece heated at 200–500 °C. The test piece was made of Inconel alloy 625 or sapphire. The shape of the Inconel alloy 625 was a disk with 6 mm in thickness and with a diameter of 28 mm. The arithmetic mean surface roughness was confirmed to be within 0.3 μm. The sapphire was a 30 mm diameter disk with 2 mm in thickness. The temperature of the solid surface was maintained at a preset value with the use of a temperature controller. The deviation from the preset temperature during the experiments was within 20 °C. The test piece with the heater unit was mounted on a multi-axis stage. The angle of a tilt solid surface was varied from 0° to 45° from the horizontal line.

The collision behavior of drops with a solid was observed by means of two-directional flash photography

that used two digital cameras and three strobe-lights, as shown in Figure 2 [6, 8, 9]. One camera (camera A), the test piece, and a pair of flash units (flashlights A, B), were aligned horizontally to obtain side-view, double-exposed, and backlit images of the drops. The impact conditions, including pre-impact diameter of drops, impact velocity, and the elapsed time after the collision could be determined from the doubly exposed images. Another camera (camera B) and a flash unit (flashlight C) were arranged to provide bird's eye view images of the drops. A flash controller activated the three flash units independently at different preset delay times with a resolution of 1 μ s. The present photographic system could take one pair of images by Camera A and B per one impact test. The time evolution of the drop shape was followed by taking many instantaneous images of drops with various flash timings under same impact conditions. The details of the photographic system and the measurement procedure were explained in our previous works [6, 8, 9].

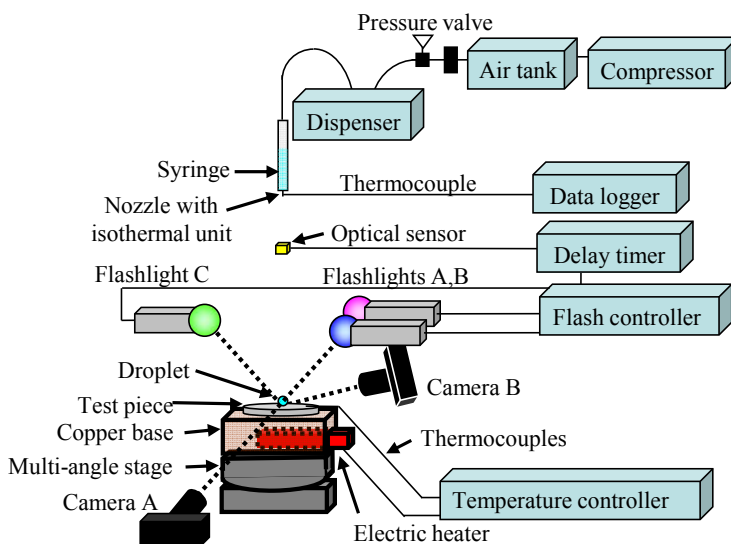


Fig. 2 Schematic diagram of the experimental apparatus and photographic setup used to observe the impact phenomena of drops

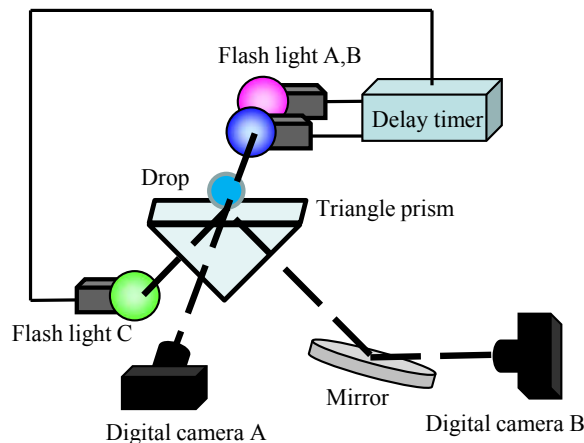


Fig. 3 Schematic diagram of the photographic system used to observe the liquid/solid interface during the drop impact

3.2 Experimental apparatus for observing the liquid/solid interface during the drop collision

Figure 3 displays the photographic alignment for observing the liquid/solid contact area during the drop collisions. The test solid was a rectangular prism made of optical glass (quartz). Three strobe lights and two digital cameras were aligned as shown in the figure. One photography system was to take doubly exposed backlit images of drops for measuring impact conditions. The other one was used to observe the liquid/solid contact area during the collision from the rear surface of the transparent prism. In the latter optical system, the incident angle of the light to the liquid/solid interface was 45°. The contact line between the water and air

on the solid can be clearly identified using this system because of the differences in the refractive indices of the two media [10, 11]. The refractive index of air (vapor), water, and quartz are 1.0, 1.33, and 1.48, respectively. Total reflection occurs at the air/glass interface, while some light passes through the water/glass interface. As the refractive index of the test solution was varied depending on the concentration of polymer and the local temperature of liquid, the boundary of the test polymer to air (vapor) was not so clear compared to the water/air interface. However, the boundary could be distinguished from the images, as will be shown later.

3.3 Definition of Weber number and estimation of interfacial temperature

The Weber number that is the ratio of the inertial force to the surface tension force, is defined by

$$We_n = \frac{\rho_l (v \cos \alpha)^2 d}{\sigma} \quad (1)$$

where ρ_l , v , d , σ , and α , are the liquid density, the impact velocity of the drop normal to the solid, the pre-impact diameter of drops, the coefficient of surface tension, and the angle of the tilt solid surface, respectively. The Weber number is a dominant parameter when the temperature of the solid is high enough to stably form a vapor layer at the liquid/solid interface [12–15].

In the present study, three types of solid materials were used, namely, sapphire, Inconel alloy 625, and quartz glass. The thermal conductivity of the quartz glass was considerably smaller than the other two materials. The difference of the thermal properties influences the temperature at the liquid/solid interface during the drop impact, even though the accurate measurement of the interfacial temperature is difficult. Instead, the temperature at the liquid/solid interface at the moment of the impact was estimated with a simple one-dimensional theory. According to the one-dimensional transient heat conduction theory for interfacial contact between two semi-infinite solids at different temperatures [16, 17], the interfacial temperature, T_i , is given by

$$T_i = \frac{T_l \sqrt{\rho_l C_l \lambda_l} + T_s \sqrt{\rho_s C_s \lambda_s}}{\sqrt{\rho_l C_l \lambda_l} + \sqrt{\rho_s C_s \lambda_s}} \quad (2)$$

where T_l , T_s , ρ_l , ρ_s , C_l , C_s , and λ_l , λ_s , are the temperatures, densities, specific heats, and thermal conductivities, of the two materials l and s , respectively. Eq. (2) was obtained by neglecting the effects of convection and phase changes. The equation can be used for rough evaluations of the interfacial temperature at the moment of the drop impact. The estimated interfacial temperatures were approximately 437 °C, 430 °C, and 300 °C, for Inconel alloy 625, sapphire, and quartz glass, respectively, when the temperature of the solid was 500 °C. The interfacial temperatures for Inconel alloy 625 and sapphire were similar to each other, but that for quartz glass was much smaller than the others.

4 Results and discussion

4.1 Collision of drops with an Inconel alloy surface at various temperatures

The collision phenomena of drops at the Inconel alloy surface at various temperatures of the solid are shown in Figures 4 to 7. All images were taken with camera B shown in Figure 2. The experimental conditions are listed in Table 1. The elapsed time after the drop impact was represented in each image. In the case of Figure 4, where the temperature of the solid was $T_w=200$ °C, the drop impacted on the solid at 0 ms, spread radially outward, and deformed into a thin circular disk. Eventually, the liquid was deformed into a dome-shaped mass. Many vapor bubbles were nucleated in the droplet through the collision. At 2.15 and 5.00 ms, the center area of the disk-shaped drop was dry owing to the blow out of a large bubble. At later times, liquid became clouded because the liquid was heated above the cloud point.

Table 1 Experimental conditions

Figure	Test solid	Solid temperature	Interfacial temperature	Pre-impact diameter	Impact velocity	We _n	Tilt angle
Fig. 4	Inconel	200 °C	190 °C	2.3 mm	0.91 m/s	39	0°
Fig. 5	Inconel	300 °C	259 °C	2.3 mm	0.91 m/s	39	0°
Fig. 6	Inconel	400 °C	347 °C	2.3 mm	0.92 m/s	39	0°
Fig. 7	Inconel	500 °C	437 °C	2.4 mm	0.83 m/s	32	0°
Fig. 8	Sapphire	500 °C	430 °C	2.3 mm	0.86 m/s	32	15°
Fig. 9	Sapphire	500 °C	430 °C	2.2 mm	1.0 m/s	34	30°
Fig.10	Quartz	500 °C	300 °C	2.3 mm	1.1 m/s	55	0°

Figure 5 shows the experimental results for $T_w=300$ °C. The liquid spread maximally and extended in the shape of a disk, constricted, and elongated upwards. The liquid was in direct contact with the solid during the entire deformation stage.

Figure 6 represents the results for $T_w=400$ °C. Many secondary droplets were generated after the impact (at 1.12 and at 1.92 ms). A bulge could then be seen at the center of the spread drop after 1.92 ms. The drop broke up into small droplets, and eventually most of them rebounded off the solid surface.

Figure 7 shows the results for $T_w=500$ °C. It is noted that the Weber number was a little smaller than the previous results. The drop impacted on the solid surface, and then spread radially. The liquid film reached its maximum extension, and then constricted. A bulge could also be seen at the center of the spread drop (2.37 ms). The liquid was elongated upwards in the shape of a bowling pin and rebounded off the heated surface (12.9 ms). The shape of the drops was roughly axisymmetric, unlike the results elicited at $T_w=400$ °C.

In our previous paper [6], the deformation process of the drops on a smooth sapphire solid was investigated using the same test solution. By comparing the results in our prior study with the present data, it was found that the motion of the drops on the Inconel alloy 625 and the sapphire showed similar tendencies.

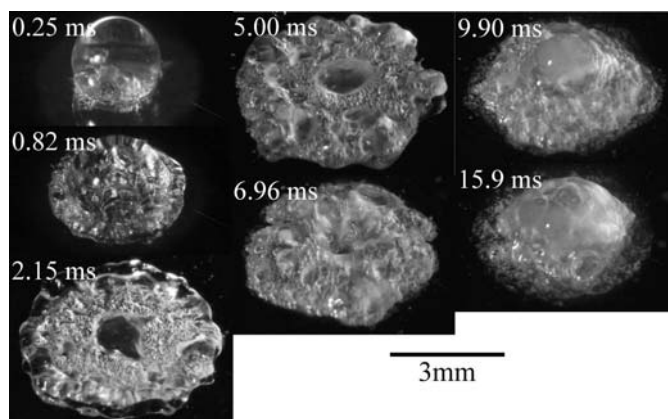


Fig. 4 Deformation behavior of drops impacting on the Inconel alloy 625 surface at $T_w = 200$ °C

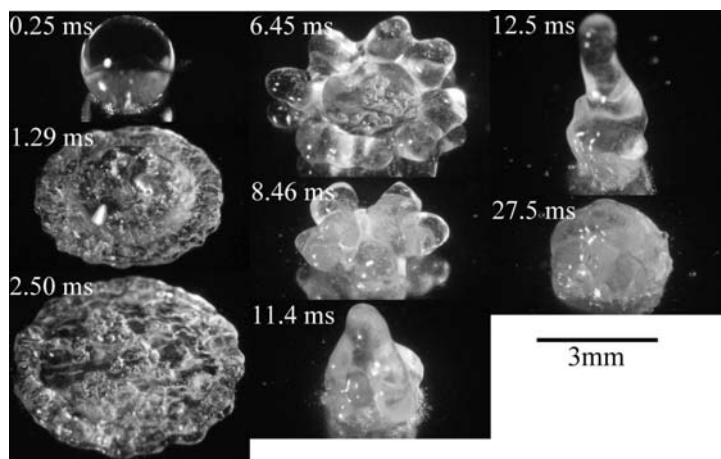


Fig. 5 Deformation behavior of drops impacting on the Inconel alloy 625 surface at $T_w = 300\text{ }^\circ\text{C}$

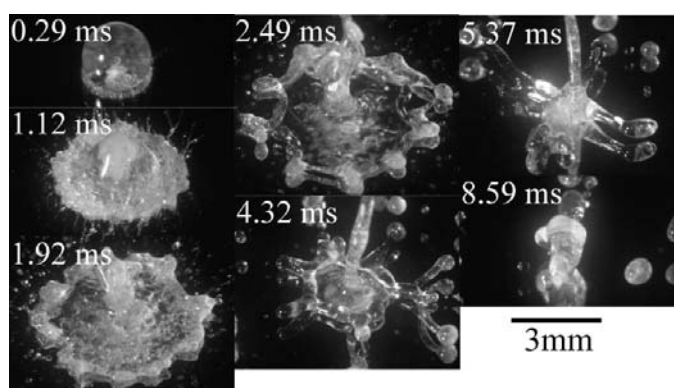


Fig. 6 Deformation behavior of drops impacting on the Inconel alloy 625 surface at $T_w = 400\text{ }^\circ\text{C}$

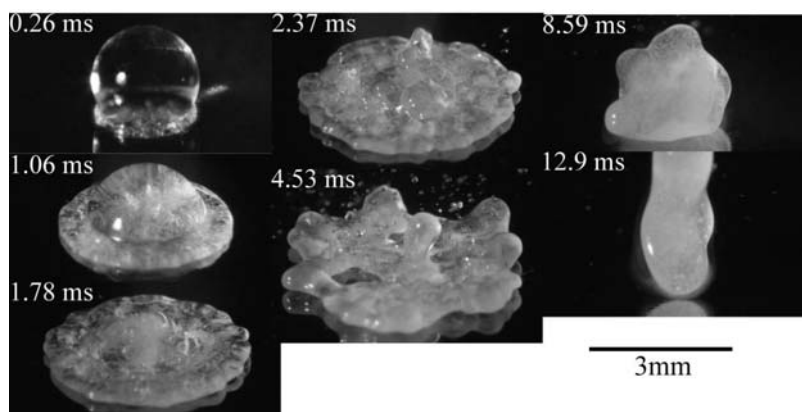


Fig. 7 Deformation behavior of drops impacting on the Inconel alloy 625 surface at $T_w = 500\text{ }^\circ\text{C}$

4.2 Effects of varying the impact angle on the collision phenomena at T_w of 500 °C

If the drops have the form of a simple liquid compound like water, and the temperature of the solid is high enough to form a vapor layer between the solid and the deforming drop, the Weber number, defined by Eq. (1), is a key parameter for the motion of the drops [9, 12–15]. For example, the residence time of the drop from the impact to the rebounding off instance can be roughly correlated by a function of the Weber number alone. In our previous work [6], we found that the measured residence times for aqueous solution drops of the polymer were slightly longer than some experimentally determined formulae [13–15]. In that work we

showed that the polymer separated from the water that was in contact with the solid, that led to a large wall friction, resulting in longer residence times. In order to confirm this mechanism by experiments, the oblique collision of drops with a solid was implemented. If the drops are insulated from the solid through a thin vapor layer, the motion of the drops could be roughly axisymmetric because of the small viscous wall friction [9]. Otherwise, the liquid motion became asymmetric owing to the wall friction.

The effect of varying the impact angle of the drops on the collision phenomena was investigated under the conditions at which the test solid was sapphire and the temperature of the solid was $T_w=500$ °C. The Weber number was approximately 32. Figures 8 and 9 represent the results for $\alpha=15^\circ$ and 30° , respectively. Other conditions are listed in Table 1. Double-exposure backlit images of drops captured by camera A are shown (see Figure 2). In Figure 8, the drop spread radially, reached its maximum extension (3.49 ms) and then constricted. A bulge can be seen at the center of the spread drop (3.49 ms). At time instants between 10.4 and 14.6 ms, the drop rebounded off the heated surface. In addition, the point at which the drop rebounded off was located farther away from the impact point because of the oblique collision. The motion of the drops in Figure 9 showed similar trends to those observed in the case of $\alpha=15^\circ$. In both cases, the shape of the rebounding drops was moderately axisymmetric. When the liquid was deformed in a disk shape, the liquid was apparently asymmetric compared to the cases of normal collision shown in Figure 7. It is also noted that the liquid shape was appreciably asymmetric for a larger solid tilt angle. In the case of $\alpha=45^\circ$, the drop motion was no longer axisymmetric, although the results are not shown. The results suggested that the polymer/solid contact occurred locally.

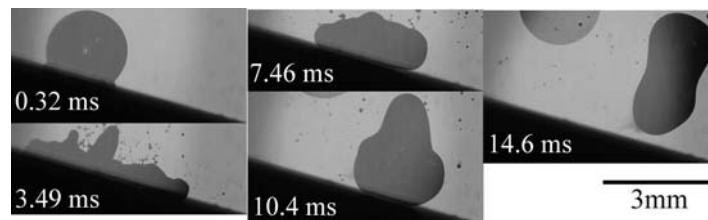


Fig. 8 Deformation behavior of drops obliquely impacting on sapphire at $T_w = 500$ °C

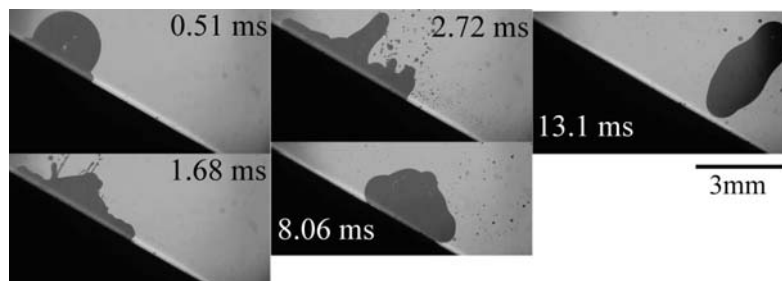


Fig. 9 Results for $\alpha=30^\circ$

4.3 Observation of liquid/solid interface during drop collision

Figure 10 represents the time variation of the liquid/solid interface captured by camera B, shown in Figure 3. The test solid was a prism made of quartz glass and the temperature of the solid was $T_w = 500$ °C. In the figure, air or vapor areas were exposed and had bright intensities because of the occurrence of the total reflection of the light. The area where the aqueous solution of the polymer was present was exposed but had dark intensities. In addition, the polymer that separated from water was not so dark compared to the aqueous solution. As previously explained, when the test solid was quartz glass, the estimated interfacial temperature was considerably lower than the cases of sapphire and Inconel alloy 625. As a result, no rebounding phenomena of drops occurred, and the liquid was in contact with the solid during the entire deformation stage. The liquid/solid direct contact area increased with time (0.52–2.39 ms). The separated polymer film from the water was observed. At later times (3.99–28.0 ms), dark areas associated with the solid/test solution contact areas were consistently present because the local interfacial temperature was decreased. Moreover,

many small, dry areas, corresponding to vapor bubbles appeared.

It is considered, based on the results of Figure 1, that the polymer film was thermally decomposed at interfacial temperatures higher than approximately 400 °C. Because of the restriction of the present experimental setup, the experiments with solid temperatures higher than 500 °C could not be conducted. This remains a challenge for future studies.

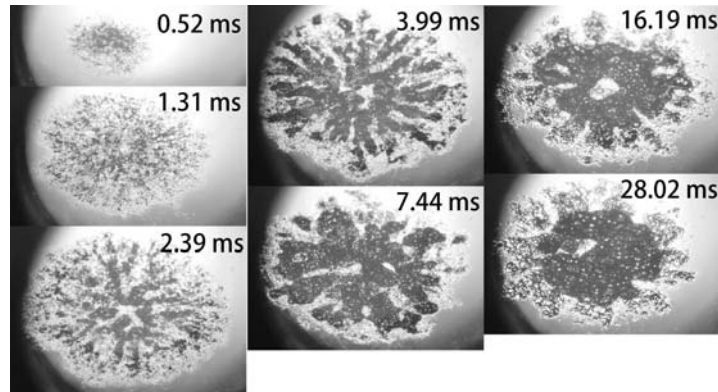


Fig. 10 Time evolution of liquid/solid contact area taken by camera B shown in fig. 3

5 Conclusions

The collisions of drops of an aqueous polymer solution with a hot surface were studied experimentally. The results obtained in the present study are summarized as follows:

- (1) The collision behavior of drops with Inconel alloy 625 surface was investigated by varying the temperature of the solid. The motion of the liquid elicited similar trends to the results that used a sapphire plate as indicated in [6].
- (2) The influence of the impact angle was studied in the case where the temperature of the solid was 500 °C. The drop showed an asymmetric motion for a larger tilt angle of the solid, suggesting that the direct contact of the solid/polymer occurred locally.
- (3) The time evolution of the liquid/solid direct contact area was observed. It was found that a separated polymer layer from water was formed during the collision.

Acknowledgement

The present work was supported by JSPS KAKENHI Grant Number 15K05825. The authors are grateful to Mr. Shohei Watanabe for his generous assistance in the experiments.

References

- [1] Totten GE, Bates CE, and Clinton NA (1993) Handbook of quenchants and quenching technology. ASM International.
- [2] Sinha AK and Division BP (1991) ASM Handbook, Volume 4: Heat Treating. ASM International, pp 601–619.
- [3] Rein M (1993) Phenomena of liquid drop impact on solid and liquid surfaces. *Fluid Dynamic Research*, vol. 12, pp 61–93.
- [4] Rein M (2002) Interactions between drops and hot surfaces, in drop-surface interactions. *CISM Courses and Lectures*, no. 456, Springer-Verlag, New York, pp 185–217.
- [5] Yarin AL (2006) Drop impact dynamics: splashing, spreading, receding, bouncing.... *Annual Review of Fluid Mechanics*, vol. 38, pp 159–192. doi: 10.1146/annurev.fluid.38.050304.092144.

- [6] Fujimoto H, Watanabe S, Okamoto T, Hama T, Takuda H (2015) Photographic study of hydrodynamics of drops aqueous polymer solution impinging on hot solid. *Experimental Thermal Fluid Science*, vol. 60, pp 66–74. doi:10.1016/j.expthermflusci.2014.08.010
- [7] Freeman PI, Rowlinson JS (1960) Lower critical points in polymer solutions. *Polymer*, vol. 1, pp 20–26.
- [8] Fujimoto H, Oku Y, Ogihara T, Takuda H (2010) Hydrodynamics and boiling phenomena of water droplets impinging on hot solid. *International Journal of Multiphase Flow*, vol. 36, pp 620–642. doi:10.1016/j.ijmultiphaseflow.2010.04.004
- [9] Fujimoto H, Doi R, Takuda H (2012). An experimental study on the oblique collisions of water droplets with a smooth hot solid. *Transactions of ASME Journal of Fluids Engineering*, vol. 134, art. no. 71301. doi:10.1115/1.4006926
- [10] Fujimoto H, Takuda H (2004). Entrapment of air at 45 degrees oblique collision of a water drop with a smooth solid surface at room temperature. *International Journal of Heat and Mass Transfer*, vol. 47, pp 3301–3305. doi:10.1016/j.ijheatmasstransfer.2004.02.029
- [11] Fujimoto H, Shiotani Y, Tong A, Hama T, Takuda H (2007). Three-dimensional numerical analysis of the deformation behavior of droplets impinging onto a solid substrate. *International Journal of Multiphase Flow*, vol. 33, pp 317–332. doi:10.1016/j.ijmultiphaseflow.2006.06.013
- [12] Wachters LHJ, Westerling NAJ (1966). The heat transfer from a hot wall to impinging water drops in the spheroidal state. *Chemical Engineering Science*, vol. 21, pp 1047–1056.
- [13] Ueda T, Enomoto T, Kanetsuki M (1979). Heat transfer characteristics and dynamic behavior of saturated droplets impinging on a heated vertical surface. *Bulletin of JSME*, vol. 22, pp 724–732.
- [14] Akao F, Araki K, Mori S, Moriyama A (1980). Deformation behaviors of a liquid droplet impinging onto hot metal surface. *Transaction of Iron Steel Institute Japan* vol. 20, pp 737–743.
- [15] Hatta N, Fujimoto H, Kinoshita K, Takuda H (1997). Experimental study of deformation mechanism of a water droplet impinging on hot metallic surfaces above the Leidenfrost temperature. *Transaction of ASME Journal of Fluids Engineering*, vol. 119, pp 692–699. doi:10.1115/1.2819300
- [16] Carslaw HS and Jaeger JC (1959) *Conduction of Heat in Solids* 2nd Edition, Oxford University Press, Oxford, p 88.
- [17] Eckert ERG and Drake RM Jr. (1972) *Analysis of Heat and Mass Transfer*, McGraw-Hill, New York, pp 158–166.